

Institutionen för systemteknik

Department of Electrical Engineering

Examensarbete

Implementation and Analysis of Spectrum Sensing Algorithms for SIMO Links

Examensarbete utfört i Kommunikationssystem
vid Tekniska högskolan i Linköping
av

Techin Eamrursiri

LiTH-ISY-EX--13/4696--SE

Linköping 2013



Linköpings universitet
TEKNISKA HÖGSKOLAN

Implementation and Analysis of Spectrum Sensing Algorithms for SIMO Links

Examensarbete utfört i Kommunikationssystem
vid Tekniska högskolan i Linköping
av


Techin Eamrursiri

LiTH-ISY-EX--13/4696--SE

Handledare: **Anton Blad**
isy, Linköpings universitet

Examinator: **Danyo Danev**
isy, Linköpings universitet

Linköping, 14 June, 2013

	Avdelning, Institution Division, Department Division of Communication Systems Department of Electrical Engineering Linköpings universitet SE-581 83 Linköping, Sweden		Datum Date 2013-06-14
	Språk Language <input type="checkbox"/> Svenska/Swedish <input checked="" type="checkbox"/> Engelska/English <input type="checkbox"/> _____	Rapporttyp Report category <input type="checkbox"/> Licentiatavhandling <input checked="" type="checkbox"/> Examensarbete <input type="checkbox"/> C-uppsats <input type="checkbox"/> D-uppsats <input type="checkbox"/> Övrig rapport <input type="checkbox"/> _____	ISBN _____ ISRN LiTH-ISY-EX--13/4696--SE Serietitel och serienummer ISSN Title of series, numbering _____
URL för elektronisk version http://www.commsys.isy.liu.se http://urn.kb.se/resolve?urn=urn:nbn:se:liu:diva-ZZZZ			
Titel Svensk titel Title Implementation and Analysis of Spectrum Sensing Algorithms for SIMO Links Författare Techin Eamrursiri Author			
Sammanfattning Abstract <p>Cognitive radio is an autonomous transceiver that is continuously sensing the ongoing communication in its environment, it then starts the communication whenever it is appropriate. Therefore, cognitive radio helps improving the spectrum utilization of the overall communication system. However, without suitable spectrum sensing techniques, cognitive radio would fail. Hence, in this thesis we investigate and implement various spectrum sensing algorithms via software defined radio for both single antenna and multiple antenna cases. The main communication scheme that we are using is OFDM. Moreover, both computer simulations and real-world measurements, have also been done for comparison and analysis of the detector's performance. The detectors we are using are based on correlation function of the received signal and generalized likelihood ratio test with its eigenvalue. The results from the simulations and measurements are then represented as probability of missed detection curves for different signal to noise ratios. Our results show that the performance of the generalized likelihood ratio test based detectors are at least 2 dB better than the correlation based detector in our measurement. Moreover, our simulations show that they are able to outperform the correlation function detector by more than 6 dB. Although, generalized likelihood ratio test based detectors seem to be better than the correlation function based detector, it requires more computational power which may limit its practical use.</p>			
Nyckelord Keywords Cognitive Radio, Spectrum Sensing, GLRT, Multi Antenna, SIMO, OFDM			

Abstract

Cognitive radio is an autonomous transceiver that is continuously sensing the ongoing communication in its environment, it then starts the communication whenever it is appropriate. Therefore, cognitive radio helps improving the spectrum utilization of the overall communication system. However, without suitable spectrum sensing techniques, cognitive radio would fail. Hence, in this thesis we investigate and implement various spectrum sensing algorithms via software defined radio for both single antenna and multiple antenna cases. The main communication scheme that we are using is OFDM. Moreover, both computer simulations and real-world measurements, have also been done for comparison and analysis of the detector's performance. The detectors we are using are based on correlation function of the received signal and generalized likelihood ratio test with its eigenvalue. The results from the simulations and measurements are then represented as probability of missed detection curves for different signal to noise ratios. Our results show that the performance of the generalized likelihood ratio test based detectors are at least 2 dB better than the correlation based detector in our measurement. Moreover, our simulations show that they are able to outperform the correlation function detector by more than 6 dB. Although, generalized likelihood ratio test based detectors seem to be better than the correlation function based detector, it requires more computational power which may limit its practical use.

Acknowledgments

First I am heartily thankful to Royal Thai Airforce (RTAF), FMV, and Linköping University for giving me the chance and financial support to study here in Communication System. It was fun, and I am very happy that I took the chance to come here. I also would like to thank my supervisor, Dr. Anton Blad, for his guidance, patience, and encouragement from start to the end. I am really appreciating your help for taking the time to read my thesis, and I hope it wasn't that bad. Further thank to my Examiner, Associate Professor Dr. Danyo Danev, for guiding me, motivating me, and giving me many wonderful advices. I learnt many things from him.

My parents and my sisters, I know you already heard this many times, but I still would like to say it here. Thank you very much for your support and everything. It really raises my spirit and keeps me going through.

Finally, I would like to thank all my friends who always try to make many humorous jokes to cheer me up. Yes, it helps. Thank you very much.

Contents

1	Introduction	3
1.1	Motivation	3
1.2	Problem Definition and Thesis Goal	5
1.3	Thesis Overview	5
2	Communication Theory	7
2.1	Digital Communication System	7
2.1.1	Source Encoding	7
2.1.2	Channel Encoding	8
2.1.3	Modulation and Demodulation	8
2.1.4	Channel	8
2.2	Multi-Antenna Communication	9
2.3	Orthogonal Frequency Division Multiplexing	10
3	Cognitive Radio	13
3.1	Cognitive Radio	13
3.1.1	Limitation of Cognitive Radio	14
3.2	Spectrum Sensing	15
3.2.1	Energy Based Detection	16
3.2.2	Matched Filter Based Detection	16
3.2.3	Cyclostationary Detection	17
3.2.4	Cooperative Sensing	18
3.3	OFDM Spectrum Sensing	18
3.3.1	Single Antenna	18
3.3.2	Multiple Antennas	20
4	OFDM Testbed	23
4.1	OFDM Testbed	23
4.1.1	Prior Requirement	23
4.2	Simulation Testbed	23
4.2.1	Simulation - Transmitter and Receiver	23
4.2.2	Simulation - Channel	24
4.3	Measurement Testbed	24
4.3.1	Measurement - Transmitter and Receiver	24
4.4	Sensors Manager	25

5	Result	27
5.1	Simulation Results	28
5.2	Measurement Result	30
5.2.1	Measurement with Line of Sight	31
5.2.2	Measurement with Non Line of Sight	34
6	Conclusion and Future Work	37
6.1	Thesis Conclusion	37
6.2	Future Work	37
	Bibliography	39
A	Some Additional Graphs	43
A.1	NLOS Measurement	43
B	Source code	45
B.1	SIMO GLRT	45
B.2	SIMO Correlation	45

Abbreviation

AWGN	Additive White Gaussian Noise
CFAR	Constant False Alarm Rate
CFD	Cyclostationary Feature Detection
CFO	Carrier Frequency Offset
CR	Cognitive Radio
CP	Cyclic Prefix
DFT	Discrete Fourier Transform
DTV	Digital TV
ED	Energy based Detection
FDM	Frequency Division Multiplexing
GLRT	Generalized Likelihood Ratio Test
IDFT	Inverse Discrete Fourier Transform
IEEE	Institute of Electrical and Electronics Engineers
LOS	Line Of Sight
MIMO	Multiple Input Multiple Output
MFD	Matched Filter Detection
NLOS	Non Line Of Sight
OFDM	Orthogonal Frequency Division Multiplexing
PU	Primary User
PUEA	Primary User Enumeration Attack
QoS	Quality of Services
SDR	Software Defined Radio
SIMO	Single Input Multiple Output
SISO	Single Input Single Output
SNR	Signal to Noise Ratio
SSDF	Spectrum Sensing Data Falsification
SU	Secondary User
USRP	Universal Software Radio Peripheral
WRAN	Wireless Regional Area Network

List of Figures

1.1	Whitespace or spectrum hole of TV spectrum	4
2.1	A block diagram of digital communication system	7
2.2	SIMO Communication	9
2.3	OFDM Modulation	10
2.4	A figure describe characteristic of parallel small frequency of OFDM	11
2.5	Cyclic Prefix in OFDM frame structure	11
3.1	A cognitive radio scenario	13
3.2	a) a centralized cognitive radio system. b) distributed cognitive radio system. c) relay-assisted cognitive radio	18
3.3	An OFDM stream structure of single antenna OFDM spectrum sensing	19
3.4	characteristic of multi-antennas cognitive radio system	21
4.1	a) Transmitter flowchart for simulation on GNURadio b) Receiver flowchart for simulation on GNURadio	24
4.2	Channel Simulator flowchart and characteristics	24
4.3	a) Transmitter flowchart for measurements on USRP b) Teceiver flowchart for measurements on USRP	25
4.4	Inside of the sensors manager block	25
5.1	Simulation results with $N_d = 256$, $N_c = 16$, $K = 200$	29
5.2	Simulation results with $N_d = 8$, $N_c = 2$, $K = 500$	29
5.3	Floor plan for line of sight case	31
5.4	LOS-Measurement result with $N_d = 256$, $N_c = 16$, $K = 200$	33
5.5	LOS-Measurement result with $N_d = 8$, $N_c = 2$, $K = 500$	33
5.6	Floor plan for non line of sight case	34
5.7	NLOS-Measurement result with $N_d = 256$, $N_c = 16$, $K = 50$	35
5.8	NLOS-Measurement result with $N_d = 8$, $N_c = 2$, $K = 100$	35
A.1	NLOS-Measurement result with $N_d = 256$, $N_c = 16$, $K = 200$	43
A.2	NLOS-Measurement result with $N_d = 8$, $N_c = 2$, $K = 500$	44

Chapter 1

Introduction

This chapter provides motivations, goal of this thesis, and the chapter overview.

1.1 Motivation

Recently, many countries in Europe and North America regions are already transitioned to Digital TV (DTV) broadcasting instead of the traditional analog broadcasting, and many other countries in other continents are planning for the transition to DTV in the upcoming years [1]. There are several benefits of DTV over Analog TV for instance a digital channel has higher bandwidth utilization, better image and stream resolution, and provides more capacity in the same bands. Furthermore, the implementation of DTV along with the regulation from the International Telecommunications Union (ITU, ITU-R BT.1368) will allow the public to utilize the television whitespace frequency as long as there is no interference to primary DTV broadcasting (see Figure 1.1). There are two methods for sensing spectrum without interference to primary signal: spectrum sensing and geolocation.

Spectrum sensing is a technique with high flexibility and robustness for the detector. The spectrum sensing detector autonomously and continuously determines the presence of the primary signal around its environment by itself. However, spectrum sensing detection can be subject to hidden terminal problem, which happens when there is an obstruction between primary user and secondary user, resulting in a scenario where a secondary user is unable to detect the ongoing signal between primary user, hence causing a collision and interference [2]. Geolocation is another method to determine available frequencies given a specific time and location. Authorities or license holders create a database containing location, device type, service area along with transmitted power, frequencies, and location of all transceiver in the same network. It is better than spectrum sensing in terms of speed and low complexity because of the provided database. However, the database has its downside due to its inflexibility to change of the environment and requires frequent updates. In addition, the devices also need suitable level of accuracy of its own location otherwise the error would be too high. Other downside

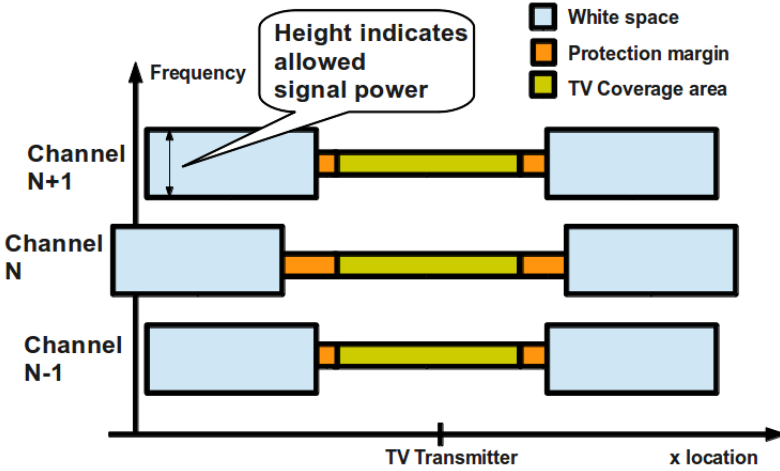


Figure 1.1. Whitespace or spectrum hole of TV spectrum

of the database is that it needs to access the database via direct-wired link or a wireless link connection. Thus, there are problems such as installation cost and interference from second spectrum.

An example of cognitive radio in the IEEE wireless standard is the Wireless Regional Area Network (WRAN) which is a technology in IEEE 802.22 standard and focuses on rural areas. It is trying to utilize the TV whitespace spectrum, which is available from 54 to 862 MHz, to its highest efficiency. For example, we can transmit an Internet broadband connectivity to the countryside together with TV spectrum [3]. The main advantage of WRAN is its large coverage area, for it can be extended to 100 Km [4] in spite of less data rate. In [5], it is stated that WRAN is better than IEEE 802.16e standard (also known as WiMax) in terms of utilization and coverage area. The table 1.1 [4] shows a WRAN requirement for

	ATSC	NTSC	Part 74
Sensing Requirement (dBm)	-116	-94	-107
Bandwidth (MHz)	6	6	0.2
SNR (dB)	-22.2	-0.2	1.5

Table 1.1. IEEE 802.22 WRAN Cognitive Radio Requirement

each type of DTV standards.

Software Defined Radio (SDR) is a radio communication technology that is implemented in software instead of hardware. Software based radio devices provide more efficient solution than the traditional hardware based because of its flexibility and modifiability to any kind of situation. The use of SDR technology enables us to implement complex algorithms, which are usually different and expensive to

implement in hardware [6]. For example, GNU Radio is a free open source software library and toolkit for SDR. It is used for implementation of radio communication by a provided signal processing library. GNU Radio was built on top of Python and C++ programming languages [7].

Another interesting wireless technology is Single Input Multiple Output (SIMO), in which the transmitter has a single antenna while the receiver has multiple antennas. Moreover, with SDR and Universal Software Radio Peripheral (USRP) from Ettus Research [8], the implementation and simulation of cognitive radio system can be conveniently implemented. As a result, it is quite interesting to simulate spectrum sensing between devices with USRP and SDR in SIMO system while observe and measure the outcome.

1.2 Problem Definition and Thesis Goal

This thesis is focusing on implementation and analysis of spectrum sensing algorithms for SIMO scenario with SDR. The implemented algorithms in this thesis are generalized likelihood ratio test (GLRT) and space-correlated detector for SIMO links. The thesis provides analysis based on computer simulation and real-time measurement with USRP. Computer simulation is representing the ideal case for the primary signal with Additive White Gaussian Noise (AWGN). On the other hand, real-time measurements with USRP are representing the simplified version of a practical situation with reduced complexity. Finally, an investigation of complexity and performance for both detectors have also been done.

1.3 Thesis Overview

Chapter 2 focuses on the necessary communication theory required to understand the later chapters.

Chapter 3 is a section on cognitive radio, which describes the current spectrum sensing methods. Most of the methods in this section are explained in detail by providing method characteristic, advantages and disadvantages, and mathematical equation.

Chapter 4 is a section on OFDM testbed and algorithm from chapter 3 implementation. The structure of the program, how it works and the difference between simulations and measurements are described in this section.

Chapter 5 contains results and discussion of the simulations and measurements from the OFDM testbed.

Chapter 6 represents the thesis conclusion and our suggestions for future work.

Chapter 2

Communication Theory

2.1 Digital Communication System

Digital communication is a transfer of digital data from one point to another point in space or time via the communication medium (see Figure 2.1). The information can be anything in any standard digital formats such as voices, videos, images, etc. However, this digital data must be converted to a sequence of discrete values first before transmission. There are several benefits of using digital communication for instance more information capacity, higher data security, and better quality.

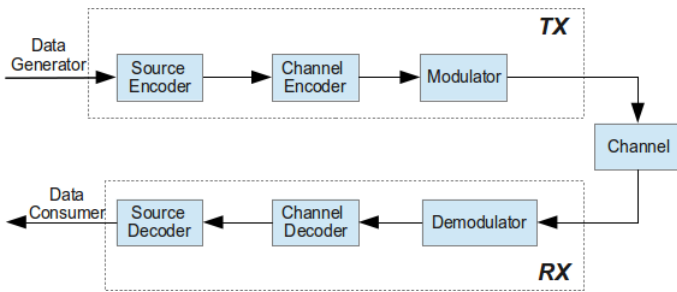


Figure 2.1. A block diagram of digital communication system

2.1.1 Source Encoding

The main objective in communication is sending an information from the transmitter to the receiver. However, we can not do the transmission directly otherwise there is too much information need to be sent. Hence, a solution to this problem needs to be implemented. Source coding is a solution to this problem in a practical setting, by reducing the redundancy of the information and efficiently representing in digital bits form, resulting in the lowest possible data rate [9]. In other words, data compression.

2.1.2 Channel Encoding

Channel coding further increases resistance to the fading of the channel by adding specific redundant data bits to the message. Thus, the receiver is able to detect or correct some errors (error detection and error correction) that occur in the channel based on the added redundant bits. There are many types of channel coding techniques for instance convolution code, block code, and cyclic code.

2.1.3 Modulation and Demodulation

Modulation is the process of translating the digital signal into an analog waveform which is more suitable for transmission over the physical channel. It is done by varying digital data over amplitude, phase, or frequency of a periodic waveform with particular carrier frequency.

2.1.4 Channel

The channel is a medium between the transmitter and receiver. It can be anything from wired physical channel such as coaxial cable, twisted pair, or fiber optic, up to wireless channel, which transmit over the air. The wireless channels in practice are particularly dynamic and affected by many natural influence such as multipath fading or Doppler effects. Nevertheless, we cannot exactly model the real-world channel to a mathematical equation for simulation and theoretical analysis, for it has many variables need to be considered. Although, we may use models such as Additive White Gaussian Noise (AWGN) channel, Rayleigh fading channel, Rician fading channel, or Nakagami fading channel instead for a mathematical and theoretical analysis.

Additive White Gaussian Noise Channel

Additive White Gaussian Noise (AWGN) is a linear channel that adds noise to the original signal source. The added noise is a white Gaussian noise process. It is usually used to model background noise and thermal noise in the receiver. According to the central limit theorem, any larger sum of equally distributed random variables or average will have approximately Gaussian distribution. White noise is a wide sense stationary process with constant power spectral density.

Rayleigh Fading Channel

Rayleigh fading is a model where a large number of scattered and reflected signal between transmitter and receiver are considered. Hence, it effects the total received energy. It can be either flat or frequency selective fading depends on the channel characteristic, which are used in modeling the multipath propagation situation, for example, communication in an urban area or the situation without line-of-sight path. From the central limit theorem, if we have scattering and reflecting happens many times in the system then flat fading will become a Gaussian process with

zero mean. Finally, we can model the relationship between the transmitted signal and the received signal as

$$y(t) = h * x(t) + n(t) \quad (2.1)$$

where $y(t)$ is the received signal, $x(t)$ is the transmitted signal, $n(t)$ is noise, and h is zero-mean Rayleigh distributed attenuation factor. It can be noted that usually Rayleigh distribution is used for modeling the wireless communication without line of sight.

2.2 Multi-Antenna Communication

Single Input Multiple Output is a communication scheme that uses one antenna for transmitter and multiple antennas for receiver. It is a simplified version of Multiple Input Multiple Output (MIMO) scheme with only one transmitter antenna (see Figure 2.2). The benefits of SIMO and MIMO over Single Input Single Output (SISO) links are a higher data rate, better Signal to Noise Ratio (SNR), and stronger resistance to multipath fading effect. Multipath fading effect happens when there is more than one path to the receiver from the transmitter. Aside from a direct path, a reflection from obstruction also reaches the receiver as another path. As a result, the received signal is a summation of many received signals resulting in phase distortion and ISI. However, in SIMO communication scheme, there are extra antennas that provide other versions of the received signal, which can be used as extra information in obtaining the original signal.

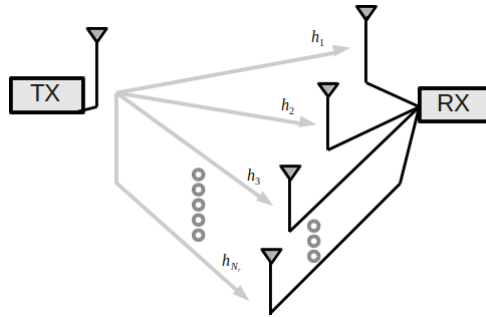


Figure 2.2. SIMO Communication

Denote N_t as the number of transmitter antennas and N_r as the number of receiver antennas. In the SIMO case, there is only one transmitter antenna which means $N_t = 1$. We define

$$H(t) = [h_1(t) \quad h_2(t) \quad h_3(t) \quad \dots \quad h_{N_r}(t)]^T \quad \text{and} \quad y(t) = H(t)x(t) + n(t), \quad (2.2)$$

where $y(t)$ and $x(t)$ are received vector and transmitted signal, H is the channel matrix with $h_i(t)$ representing each channel attenuation factor for $1 \leq i \leq N_r$, and $n(t)$ is the noise vector.

2.3 Orthogonal Frequency Division Multiplexing

Orthogonal Frequency Division Multiplexing (OFDM), which is currently a commonly use modulation scheme in communication technology, is a transmission technique for representing digital data. The benefits of the OFDM consist of high resistance to multipath fading and better spectral efficiency. Implementation of OFDM starts from splitting one big chunk high data-rate stream to N lower data rate streams, which are simultaneously transmitted. This is depicted in Figure 2.3.

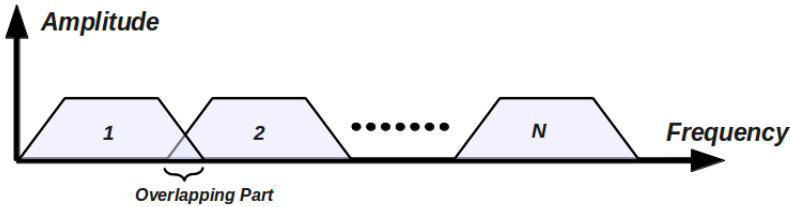


Figure 2.3. OFDM Modulation

Not only OFDM is splitting the stream into N sub streams, but the sub-carriers must be "orthogonal" to each other. Let $c_m(t)$ and $c_l(t)$ be two complex valued ergodic signals with period T . If the following is valid where $(.)^*$ denotes complex conjugation, we say that $c_m(t)$ and $c_l(t)$ are orthogonal.

$$\rho_{ik} = \int_0^T c_l(t)c_m^*(t)dt \begin{cases} 1, & l = m \\ 0, & l \neq m \end{cases} \quad (2.3)$$

In general, the whole process of OFDM modulation is as follows (see figure 2.4). First, it starts from the digital data signal x_n modulated by some digital modulation scheme and mapped to a constellation point to create complex symbol \tilde{d}_n . Next the sequence of symbols pass through size N_d -IDFT to transfer it to complex value time domain signal. Furthermore, by adding cyclic prefix of length N_c to those symbols for every block of symbols of length N_d , we can removes Inter Symbol Interference (ISI) caused by the fading channel. Finally, both real and imaginary parts of the signal are converted to analog signals and modulated with sinusoidal wave at some carrier frequency f_c . Cyclic prefix is a prefixing method of adding the end of the symbol block in front of the symbols as a guard time (see figure 2.5). To mathematically explain OFDM, start with the IDFT of the

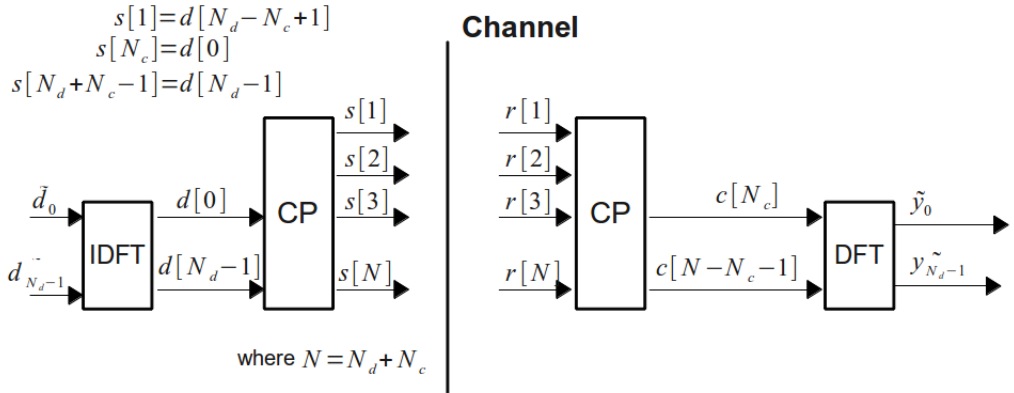


Figure 2.4. A figure describe characteristic of parallel small frequency of OFDM

mapped symbols [10]

$$d[n] = \sum_{m=0}^{N_d-1} \tilde{d}_m e^{j2\pi mn/N_d}, \tag{2.4}$$

where \tilde{d}_m is a modulated symbol. Additionally, we then add a N_c symbols long cyclic prefix to the output from IDFT to avoid the ISI to obtain the vector.

$$\mathbf{s} = [d[N_d - N_c + 1], d[N_d - N_c + 2], \dots, d[N_c - 1], d[0], \dots, d[N_d - 1]]^T \tag{2.5}$$

The vector \mathbf{s} now becomes an input block of length N which equals to $N_c + N_d$. Moreover, we would like to send this over the channel. Assume that the received signal from the channel equals to $r[n]$ for $0 \leq n \leq N - 1$. The receiver then demodulates the received stream and sends it through the filter to remove cyclic prefix which results in $c[n]$, where the block length equals to N_d . Thereafter, by taking the DFT of received signal $c[n]$, it converts from time domain back to frequency domain which after symbol mapping restores the original data signal \tilde{y}_m .

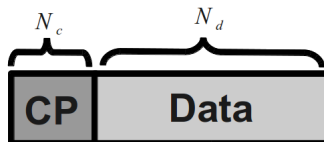


Figure 2.5. Cyclic Prefix in OFDM frame structure

Chapter 3

Cognitive Radio

3.1 Cognitive Radio

Most receivers nowadays are not aware of their surrounding leading to inability to maximum utilization of the available spectrum. Cognitive radio (CR) systems are capable of detecting the signal transmission in their surroundings and acting accordingly to prevent interference. Opportunistic spectrum access is a cognitive radio concept of accessing an unused part of the spectrum without any impact on that specific primary signal [11]. Normally, the primary user (PU) who transmits the primary signal is not always utilizing the whole spectrum band, for it has idle periods. The idle period of the PU allows other users to access the spectrum. This is known as spectrum hole or as whitespace frequency. As a result, opportunistic spectrum access increases the efficiency of spectrum utilization. The receiver that adapts the opportunistic spectrum access concept is a secondary user in a CR system. In short, CR is an intelligence transceiver which is able to automatically switch to available channels. Figure 3.1 is describing the scenario using cognitive radio.

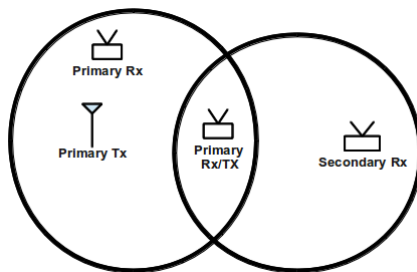


Figure 3.1. A cognitive radio scenario

There are four functionalities of CR network. These are spectrum sensing,

spectrum management, spectrum mobility, and spectrum sharing [12]. Spectrum sensing is a task responsibility of the secondary users. A secondary user must sense the ongoing primary signal transmission. This will be explained in Section 3.2 in detail. Spectrum management [13] is a set of rules for all devices in the network in order to achieve acceptable quality of service. For example, the CR devices are aware of the overall effect to the quality of service of the channel, and they should provide a seamless communication even though the PU is not present. Next, spectrum sharing is a scheme to coordinate the access of each CR device in the CR network to the available spectrum. That is needed because, generally, we always have more than one CR devices in the network. Thus, there is a chance that many CR devices try to access the spectrum at the same time resulting in collisions which destroys the signals. The last function is spectrum mobility. Because a CR device is a secondary user (SU) in a CR network, it needs to hop and continue communication in the other available resource when the currently used spectrum is required by the primary user.

3.1.1 Limitation of Cognitive Radio

Aside from increasing the spectrum utilization with cost effectiveness, CR also enables a reliable communication for every user in the CR network. Nevertheless, there are three major limitations of CR; hidden terminal problem, security risk, and burden of control [14].

Hidden Terminal

Hidden terminal problem happens when a CR device is unable to detect the primary signal from a PU due to the distance between them or low signal strength. Consequently, the CR device decides to use this spectrum because it thinks this spectrum is available which, in reality, is not. As a result, the CR device interferes the communication of the PU.

Security Risk

Security risk is another problem in CR networks [15] that needs to be looked at. The first security problem is a Primary User Emulation Attack. It explains the situation when an attacker mimics itself as a PU which then transmits a fake primary signal. Hence, both SU and CR devices detect a fake primary signal, and hop to the other spectrum. Thus, the attacker greedily uses this spectrum as its own exclusive spectrum, and it disrupts the entire CR operation, and violates spectrum management's unfairness policy. The next security problem is Spectrum Sensing Data Falsification. It is a problem occurring in cooperative spectrum sensing CR networks (see section 3.2.4) when there are one or more SUs providing false decisions, intentionally or not. For example, some SUs always report the channel is available even though it is occupied by a PU. The effect of this to the whole CR network is surprisingly high. In [16], it is claimed that just one intended SU can severely decrease the overall performance and reliability of the network. Other security problems such as spoofing, congestion attack, and jamming attack arise from

the core concept of wireless security risk, due to the fact that CR is working upon wireless communication. Furthermore, most CR devices are implementing on SDR which is vulnerable to software hacking and virus.

Burden of Control

Burden of control is a limitation which prevent CR implementation in a global scale. In practice, in a very large multi nation CR network there should be some organization which is responsible for device standardization and for collaboration between the country. Therefore, this organization bears the large burden of controlling and monitoring the network, which production costs may not be compensated by the benefits of CR.

3.2 Spectrum Sensing

Spectrum sensing is a method used in detecting the ongoing wireless transmissions. There are two kinds of spectrum sensing. These are horizontal spectrum sensing and vertical spectrum sensing. Horizontal spectrum sensing gives both PU, and SU equal priority. On the other hand, vertical spectrum sensing gives PU more priority than the secondary user, and this is the technique used in CR system. Moreover, vertical spectrum sensing can be further categorized to non-cooperative sensing and cooperative sensing. Non cooperative spectrum sensing (primary transmitter detection) is a technique where the CR acts on its own based on the received signal. On the contrary, the cooperative sensing is focused on sharing information between the receivers in the CR network which is gathered in a central station. The central node then combines all received information and setting the decision rule for the network. This subsection covers non-cooperative sensing and cooperative sensing in detail. Denote H_0 as the hypothesis that PU is inactive and H_1 as the that the PU is active. This can be written as

$$H_0 : y[n] = w[n], \quad n = 0, \dots, N - 1, \quad (3.1)$$

$$H_1 : y[n] = x[n] + w[n], \quad n = 0, \dots, N - 1, \quad (3.2)$$

where $y[n]$ is the received signal in the discrete time instant n , $x[n]$ is the PU's signal at time n , and $w[n]$ is the noise. All of them have the block length of N . In order to determine the current hypothesis for each detector, we define a threshold value to separate between H_0 and H_1 by comparing it with a value metric computed for each method,

$$T_{method} \underset{H_0}{\overset{H_1}{\gtrless}} \gamma_{method}, \quad (3.3)$$

where T_{method} is the metric value found from each method's test statistics, and γ_{method} represent the threshold of each method which varies depending on the probability of false alarm. Equation (3.3) concludes that the primary signal is present when metric value is greater than threshold value, and vice versa. In addition, we define the probability of missed detection P_{MD} as the ratio between

the number of undetected symbols to the total number of transmitted symbols, and probability of false alarm P_{FA} as the probability of the detector deciding PU is active when it is not. Another perimeter need to be considered is the Constant False Alarm Rate (CFAR) which represents how much noise variance affect on the whole detector. Generally, the most suitable detector should has CFAR feature.

3.2.1 Energy Based Detection

The energy based detector (ED) is the most suitable detector and spectrum sensing technique for CR when the receiver is aware of the noise variance of the channel. This is because ED requires no prior knowledge of the signal structure of the PU signal, which in this case is the type of modulation, the time synchronization, and the pulse shaping. [17] Nonetheless, there are many downsides of the ED. First, ED is relying too much on noise variance. If the estimation of the noise variance is inaccurate, it causes a great affect on the ED detection ability [18]. Second, due to limitation of the ED on accurate sensing, ED cannot discriminate PUs from CR user in the same network. Additionally, ED in theory should be able to detect signals in direct spread spectrum, even so [19] shows that it performs poorly in classifying this type of spectrum. The equation that is used for finding the test statistics value is

$$T_{ED} = \sum_{n=0}^{N-1} |y[n]|^2, \quad (3.4)$$

The probability of false alarm has been derived in [20] to be

$$P_{FA} = 1 - P\left(\frac{\gamma_{ED}}{2}, N\right) \quad (3.5)$$

where $P\left(\frac{\gamma_{ED}}{2}, N\right)$ is the lower incomplete gamma function. It should be noted that ED is not a CFAR detector.

3.2.2 Matched Filter Based Detection

Matched Filter Detection (MFD) is a method of detecting PU when the exact primary transmitted signal are known before the communication. Matched filter is an optimal linear filter which maximizes the SNR characteristics. It calculates the level of similarity between two signals, which are the unknown incoming signal and the primary signal, by using convolution of the incoming signal and mirrored time shifted version of the primary signal, i.e.

$$b[n] = \sum_{l=-\infty}^{\infty} h[n-l]y[l], \quad (3.6)$$

where $h[l]$ is the primary signal and $y[l]$ is the received signal. The metric in this case can be then computed from the similarity between received signal and the

known signal. The threshold value of the MFD can be determined by the target false alarm, and is given [21] by the equation

$$P_{FA} = Q\left(\frac{\gamma_{MFD}}{\sigma_W\sqrt{E}}\right), \quad (3.7)$$

One advantage of the MFD is that it is very fast to target the probability of false alarm which resulting in better probability of missed detection. However, in practice the characteristics of the transmitted signal are usually unknown, resulting in unusable detector. Moreover, MFD consumes very large power resources as each detector need to be executed independently, not to mention the requirement of dedicate detector for each type of primary signal.

3.2.3 Cyclostationary Detection

Cyclostationary Feature Detection (CFD) is another sensing method, which uses the cyclostationary features of the signal. The paper [22] suggests that CFD is the best option in spectrum sensing because it does not require any prior knowledge of primary signal except the cyclostationary characteristics. Moreover, CFD is resistant to sensitive noise variance estimation. Thus, CFD in most of the case is better than both MFD and ED. It is said that the signal is cyclostationary, if it has a periodical autocorrelation function in time. The autocorrelation function is given as

$$R_{yy}[n, \tau] = E[y[n]y^*[n, \tau]], \quad (3.8)$$

where $y[n]$ is the signal. By periodicity we mean and $R_{yy}[n, \tau]$. The test statistics for the CFD detector is defined as a periodic autocorrelation function in the time n for delay parameter τ .

$$T_{CFD-CAF} = R_{yy}^\alpha[n, \tau] = \lim_{T \rightarrow \infty} \frac{1}{T} \sum_{n=-\frac{T}{2}}^{\frac{T}{2}} R_{yy}[n, \tau] e^{-j2\pi\alpha n} \quad (3.9)$$

where $R_{yy}^\alpha[t, \tau]$ is the cyclic prefix autocorrelation function (CAF) for the cyclic frequency α . Moreover, by applying FFT to CAF we will get cyclic spectrum (CS) $S_{yy}^\alpha[\tau]$ as stated in the equation.

$$T_{CFD-CS} = S_{yy}^\alpha[\tau] = \sum_{\tau=-\infty}^{\infty} R_{yy}^\alpha[\tau] e^{-j2\pi f\tau}. \quad (3.10)$$

With a given specific cyclic frequency, the detector performs spectrum sensing by comparing either CAF or CS to a given threshold γ_{CFD} . If CAF or CS is higher than γ_{CFD} , the signal is present otherwise the signal is absent. The probability of false alarm of CFD for a given threshold is derived in [20] as

$$P_{FA} = (1 - \gamma_{CFD})^L, \quad (3.11)$$

where L is the number of segmented disjoint symbols. Consequently, equation (3.11) shows that noise variance σ_w does not effect the probability of false alarm, this is the reason why CFD is robust to noise variance estimation. Furthermore, if the transmitted primary signal has a strong cyclostationary characteristic, we can detect even in low SNR condition. Nevertheless, the sensing time of CFD is long due to high computation complexity algorithm which is undesirable in practical CR networks.

3.2.4 Cooperative Sensing

Cooperative sensing is another sensing method used in today's communication. It helps reducing the multipath fading effect and the probability of false alarm by sharing information between the detectors. The information from each detector is sent to central station where it is combined and final decision for the whole network is taken. However, by increasing the number of the receivers the cost also increase as a trade off for efficiency. In [19], the cooperative sensing techniques are classified into three categories: centralized, distributed, and relay-assisted. Graphical explanation of those are given in Figure 3.2

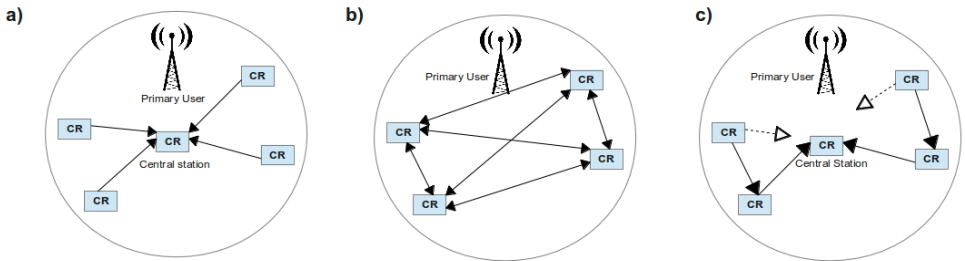


Figure 3.2. a) a centralized cognitive radio system. b) distributed cognitive radio system. c) relay-assisted cognitive radio

3.3 OFDM Spectrum Sensing

As already explained in Section 2.3, OFDM consists of data part and cyclic prefix part which have lengths N_d and N_c respectively. We first assume that the current ongoing primary signal is using OFDM modulation, and the detector already knows the block length and cyclic prefix length.

3.3.1 Single Antenna

For the single antenna spectrum sensing, we have only one received stream with unknown total size. However, by assuming that the receiver observes only K consecutive OFDM symbols, then the total size of the stream is $N_{total} = KN$ samples where $N = N_c + N_d$ (see figure 3.3). Moreover, by exploiting CP characteristic

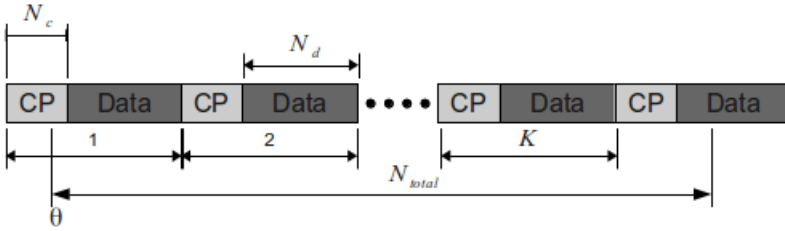


Figure 3.3. An OFDM stream structure of single antenna OFDM spectrum sensing

of OFDM we can make an assumption that there should be unique correlation structure somewhere in the sample block. Normally, the input samples are uncorrelated, but because of the added redundancy such as CP it is not the case for OFDM signals. We define autocorrelation function of $y[n]$ as

$$\hat{r}_y[n, N_d] = y[n]y^*[n + N_d], \quad 0 \leq n \leq N_{total} - 1, \quad (3.12)$$

where $\hat{r}_y[n, N_d]$ is a time varying non stationary correlation function while

$$\begin{aligned} E\{\hat{r}_y[n, N_d]\} &> 0, & \text{for } n \text{ in the CP range,} \\ E\{\hat{r}_y[n, N_d]\} &= 0, & \text{for otherwise.} \end{aligned}$$

As stated before, the added CP makes this correlation function non-zero for a period of lengths N_c , and zero elsewhere. However, because $\hat{r}_y[n]$ and $\hat{r}_y[n + N_d]$ are independent to each other, it is better to average each correlation index in the block with the same position index of other blocks which will reduce the AWGN effect of the channel. The resulting average autocorrelation function is $\hat{R}_y[n]$, and its length reduces from a total of K OFDM blocks to only one. We use this function in the sensing method describe below.

$$\begin{aligned} \hat{R}_y[n] &= \frac{1}{K} \left(\sum_{l=0}^{K-1} \hat{r}_y[n + lN] \right) \\ &= \frac{1}{K} \left(\sum_{l=0}^{K-1} y[lN + n]y^*[lN + N_d + n] \right), \quad 0 \leq n \leq N - 1. \end{aligned} \quad (3.13)$$

Average Correlation with Carrier Frequency Offset

The [23] proposed a test statistic for auto correlation based detector as

$$\frac{1}{N} \left(\sum_{n=0}^{N-1} \Re\{y[n]y^*[n + N_d]\} \right) \quad (3.14)$$

where $\Re\{\cdot\}$ denotes the real part of the complex correlation function. However, [24] suggests that by using the average correlation function instead of normal

correlation function better results can be obtained. So, we modify equation (3.14) to use $\hat{R}_y[n]$ instead of $\hat{r}_y[n]$. Moreover, because the carrier frequency offset forces the correlation function to be complex valued and not non-negative real valued, which opposes [23]'s assumption. This is why we decide to follow [24] suggestion on using absolute value instead of real value. Finally, the test statics becomes

$$T_{Average} = \frac{1}{N} \left| \sum_{n=0}^{N-1} \hat{R}_y[n] \right|, \quad (3.15)$$

for a non normalized case, and

$$T_{Average-normalize} = \frac{\left| \sum_{n=0}^{N-1} \hat{R}_y[n] \right|}{\sum_{m=0}^{N_{total}-1} |y[n]|^2}, \quad (3.16)$$

for a normalized case. Generally, we need to use the normalized detector otherwise there is a problem in signal power.

WRAN with Carrier Frequency Offset

WRAN test statistic is based on [25] which uses a sliding window of length N_c over a whole $N + N_c$ period since we need to slide over a whole OFDM symbol (N). The test statistic is then written as

$$\max_{\tau} \left| \sum_{n=\tau}^{\tau+N_c-1} r_y[n] \right|,$$

where τ is a sliding window index, such that $0 \leq \tau \leq N_c + N_d - 1$ range. Nonetheless, the proposed static only considers one OFDM symbol at a time, but with suggestions from [26] to utilize multiple symbols resulting in a better performance, the test statistics then becomes

$$T_{WRAN} = \frac{\max_{\tau} \left| \sum_{n=\tau}^{\tau+N_c-1} \hat{R}_y[n] \right|}{\sum_{n=0}^{N-1} |y[n]|^2}. \quad (3.17)$$

3.3.2 Multiple Antennas

Multiple antennas spectrum sensing is better than single antenna because SIMO and MIMO are more capable to combat fading. We consider the scenario of multi-antennas spectrum sensing in this subsection. The major difference between single antenna scenario and this scenario is that instead of only one stream, we now have multiple streams. Denote $y_i[n]$ as the received stream from the i th antenna while N_r represents number of received antennas. As in the single antenna section, we assume that one symbol of OFDM has length of $N = N_d + N_c$, where N_d and N_c are length of FFT and CP, respectively. Furthermore, we assume that we have received in total K symbols which means the total received steam length is $N_{total} = KN$. Moreover, since in practice the receiver is not synchronized, there

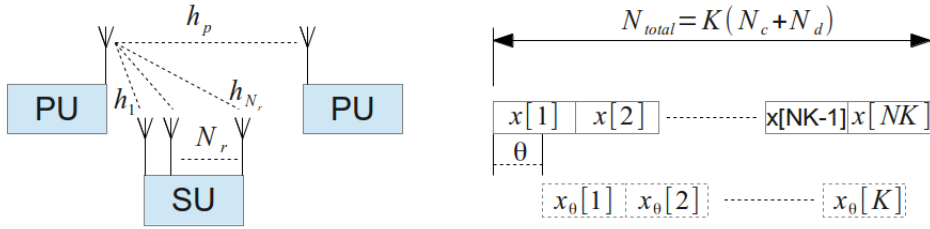


Figure 3.4. characteristic of multi-antennas cognitive radio system

is no guarantee that we have received integer number of symbols. However, by maximizing θ as a shifted offset length, where θ ranges from zero to one symbol length of OFDM ($0 \leq \theta \leq N - 1$), we can mitigate the error. We note that in the case of $\theta = 0$, this means that the receiver is synchronized.

SIMO Correlation

In this SIMO Correlation case, we neglect the synchronization error for the purpose of using this detector in the simulation. First, we create a received matrix of every streams from every antennas Y which is defined as

$$\mathbf{Y} = \begin{bmatrix} y_0(0) & y_0(1) & \cdots & y_0(N_{total} - 1) \\ y_1(0) & \ddots & & \vdots \\ \vdots & & \ddots & \vdots \\ y_{N_r-1}(0) & \cdots & \cdots & y_{N_r-1}(N_{total} - 1) \end{bmatrix} \tag{3.18}$$

and then create a sample covariance matrix R_y

$$R_y = \frac{1}{N} \mathbf{Y} \mathbf{Y}^H, \tag{3.19}$$

where \mathbf{Y}^H is the conjugate transpose of the matrix \mathbf{Y} itself. As a result from matrix multiplication, R_Y then becomes a self-adjoint $N_r \times N_r$ square matrix which is used in finding the eigenvalue. The eigenvalue and eigenvector are the method in linear algebra which provide solution to dynamic problem. The test statistics then can be found from the maximum likelihood test hypothesis derived in [17]. However, we can use eigenvalues along with the simplify version of that equation, which has less complexity, for finding test static metric instead. This can be written as

$$T_{Corr} = \frac{\max\{\lambda\}}{\sum_{m=1}^M \lambda_m}, \tag{3.20}$$

where $\max\{\cdot\}$ denotes maximum values of the vector, and λ_m are the eigenvalues of R_Y in descending order, and M is the number of eigenvalues.

SIMO Generalized Likelihood Ratio Test

In this case, we are using eigenvalue characteristics to extend GLRT in the case of synchronization error. In [27] the author suggests the sample covariance matrix which is defined as

$$\hat{R}_\theta = \frac{1}{K_\theta} \sum_{k=1}^{K_\theta} \mathbf{v}_\theta[k] \mathbf{v}_\theta[k]^H, \quad (3.21)$$

where $\mathbf{v}_\theta[k]$ is a column vectorization of received matrix Y in equation (3.18) with \mathbf{v}_θ is a received vector for each synchronization error θ , and $K_\theta = \lfloor \frac{KN-\theta}{N} \rfloor$ which in other word K_θ is equals to K when $\theta = 0$ and $K_\theta = K - 1$ for otherwise. The paper [27] further suggests that by using \hat{R}_θ to find the eigenvalue $\hat{\lambda}_{i,\theta}$ for each θ , we can find the test statistic by using following equation.

$$T_{GLRT} = \max_{\theta \in \{0,1,\dots,N-1\}} \frac{\left(\frac{1}{N_{total} N_r} \sum_{n=1}^{N_{total}} \|\mathbf{v}_\theta[n]\|^2 \right)^{N_r N}}{\prod_{i=1}^p \left(\hat{\lambda}_{i,\theta} \right)^{q_i}} \quad (3.22)$$

where p is the number of distinct eigenvalues. We consider here $p = 3$ and multiplicities $q_1 = N_c$, $q_2 = N_d - N_c$ and $q_3 = N_r(N_d + N_c) - N_d$.

Chapter 4

OFDM Testbed

4.1 OFDM Testbed

All simulations and measurements in this work have been performed on GNU-Radio. In addition, the USRPs have been used for measurement case. The core structure of the code and most of the classes are retrieved from the website [28]. We have just edited and added more thesis related classes. Moreover, the external C++ signal processing library Eigen3 [29] has also been used in this thesis. This section illustrates the flow and structure of the testbed including both simulations and measurements. There are more hidden processes of the OFDM testbed that are not covered in this section.

4.1.1 Prior Requirement

Our objective is setting up a (1x2) SIMO system by using GNU Radio and USRP. However, setting SIMO up in simulation can be done by directly separating the received stream into two streams without mathematical verification. On the other hand, measurements with USRP need to be verified by using the equation (4.1).

$$\theta = \arg \left\{ \frac{y_0[n]}{y_1[n]} \right\} \quad (4.1)$$

where $y_0[n]$ is received signal from the first antenna and $y_1[n]$ is received signal from the second antenna. If the system is a SIMO system θ must be constant for a whole period.

4.2 Simulation Testbed

4.2.1 Simulation - Transmitter and Receiver

The program starts from OFDM generator block which generates the OFDM stream by taking three values as input; FFT size, cyclic prefix length and amplitude. The output OFDM stream is then written to a file representing a string

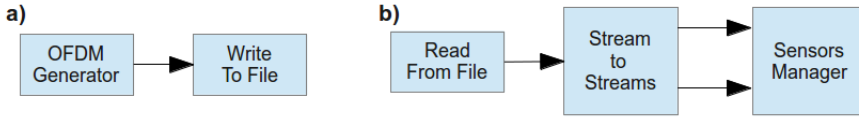


Figure 4.1. a) Transmitter flowchart for simulation on GNURadio b) Receiver flowchart for simulation on GNURadio

of complex number in a binary form. This file is read by the simulated channel routine, which is explain in the next subsection. After the file has been processed through the channel, the receiver then reads this generated file and extracts input stream into two output streams ($y_0[n]$ and $y_1[n]$). It does so by separating every other value from the original stream. Finally, both of them become inputs to the sensors manager block (see section 4.4) and continue processing by the testbed (see figure 4.1).

4.2.2 Simulation - Channel

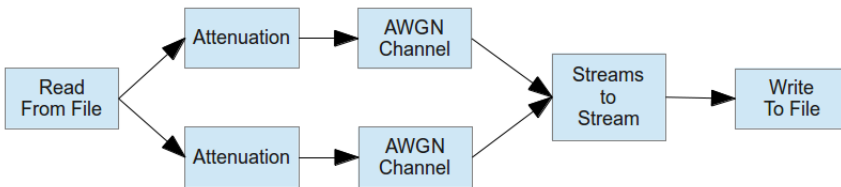


Figure 4.2. Channel Simulator flowchart and characteristics

The channel simulator starts by reading the previous saved file from the transmitter then duplicates it into two streams. This is because we need to use different seed for each stream so that output from pseudo random number generator for both channel are independent. Thereafter, both streams are attenuated and pass through an AWGN channel with different seed and finally combined into one stream. (see figure 4.2)

4.3 Measurement Testbed

4.3.1 Measurement - Transmitter and Receiver

After the OFDM has already been generated by the OFDM generator block, we transmit the data via the USRP with specific center frequency, data rate, FFT size, and CP length. The USRP automatically handles the modulation and demodulation from the center frequency. However, we still need to consider the time synchronization of both USRPs. So, the detectors must handle the frequency offset from the channel (see figure 4.3).

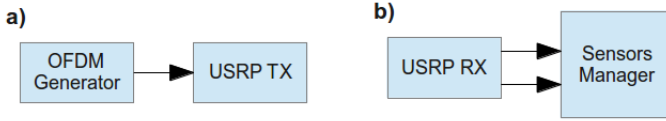


Figure 4.3. a) Transmitter flowchart for measurements on USRP b) Teceiver flowchart for measurements on USRP

4.4 Sensors Manager

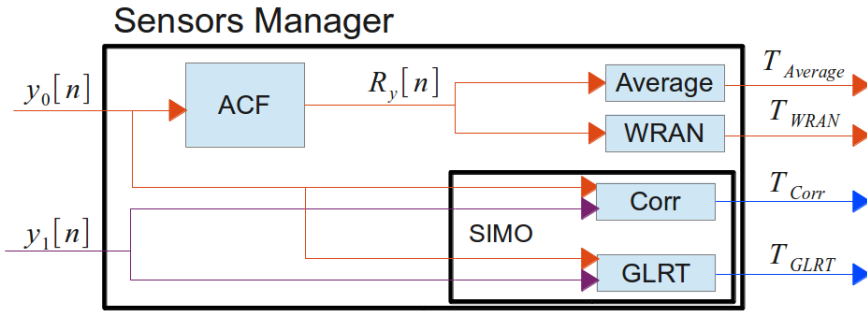


Figure 4.4. Inside of the sensors manager block

This is the block that do the algorithms described in Chapter 3. There are 4 types of sensors that we are using in the simulations and measurements; average correlation function detector (section 3.3.1), WRAN detector (section 3.3.1), SIMO Correlation detector (section 3.3.2), and SIMO GLRT detector (section 3.3.2). First, the sensors manager block has two inputs which represents each of the streams from the antennas, $y_0[n]$ and $y_1[n]$. However, both Average correlation detector and WRAN detector need to use autocorrelation function (ACF). So, one of the stream need to be an input for the ACF block, which in this case is $y_0[n]$. The ACF block then calculates the ACF, and its average correlation function $R_y[n]$ from $y_0[n]$ according to equation (3.13). Next, the output from the ACF block goes to both the Average and WRAN block as an input. On the other hand, both SIMO blocks require both unprocessed streams ($y_0[n]$ and $y_1[n]$) as input. Finally, the result from the each block is the test statistics metric T which is compared to a threshold value γ .

Chapter 5

Result

As explained in section 4.2, we are performing simulations for detector performance comparison by calculation the probability of missed detection for various values of the SNR. The probability of missed detection can be computed from the number of missed detections N_{miss} divided by number of total transmissions which equals to $(N_{pos} + N_{miss})$. The equation can be written as

$$P_{MD} = \frac{N_{miss}}{(N_{pos} + N_{miss})}. \quad (5.1)$$

The simulations and measurements are run by another Python evaluation program which starts from measuring the noise to create a reference SNR then using the SNR values to derive decision threshold from the experiment base on noise only samples. Moreover, the evaluation program is further calibrated to achieve a target false alarm $P_{FA} = 0.05$. All of these steps are done automatically by the evaluation program from OFDM testbed [28]. Finally, the probability of missed detection from equation (5.1) against the SNR were obtained as a result.

5.1 Simulation Results

Figure 5.1 shows the probability of missed detection for Average correlation detector(section 3.3.1), WRAN detector(section 3.3.1), and SIMO Correlation detector(section 3.3.2). The setting consist of $N_d = 256$, $N_c = 16$, and $K = 200$.

The setting for the results in Figure 5.2 are almost the same as those for figure 5.1 except that there are four detectors which are Average correlation detector, WRAN detector, SIMO Correlation detector, and SIMO GLRT detector(see section 3.3.2), instead. Other difference are the value of the N_d , N_c , and K , which have been reduced to $N_d = 8$, $N_c = 2$ and $K = 200$, respectively.

From both figures we can clearly see that the SIMO GLRT detector outperforms other detectors, for it approaches zero fastest with approximately 7 dB and 13 dB difference when compared with the WRAN detector and the Average correlation detector respectively. Moreover, WRAN detector is also working better than the Average correlation detector with about 6 dB. In Figure 5.2, we add another detector which is the SIMO GLRT detector. According to it, this detector is working slightly better than the SIMO Correlation detector with about 1 dB. However, we have not verified the result with larger N_d and N_c due to algorithm complexity limitation. We note that the performance difference between the detector in Figure 5.2 is less than the difference in Figure 5.1. For example, the difference between the Average correlation detector and the WRAN detector reduce from 6 dB to 4 dB. Finally, both results are accordingly following the reference papers [24],[27], which to some extent verifies our implementation.

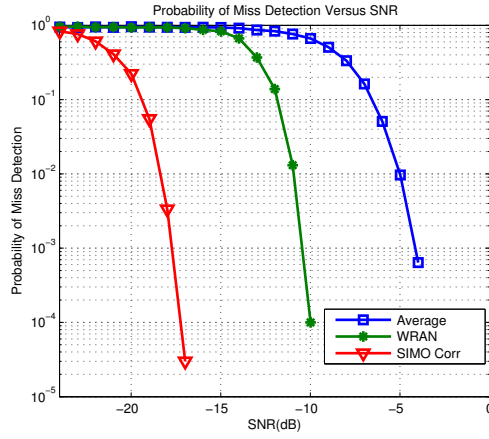


Figure 5.1. Simulation results with $N_d = 256$, $N_c = 16$, $K = 200$.

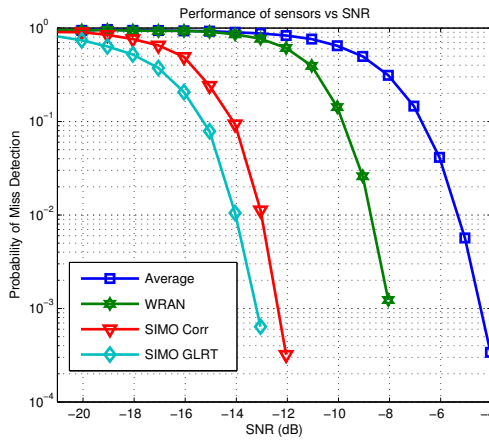


Figure 5.2. Simulation results with $N_d = 8$, $N_c = 2$, $K = 500$.

5.2 Measurement Result

In the measurement case, we are performing measurements in an indoor concrete room of size 20×10 m shielded from Wireless LAN interference. Furthermore, this room was also crowded by many obstacles such as Personal Computer (PC) case, bicycles, cabinets, etc. The measurements were done on a single PC connected with two USRPs, one for the PU which transmits OFDM signal, and another one for the SU which continuously senses the ongoing signal. The two receiver antennas were placed side by side near the wall while the transmitter antenna was placed at the corner of the room. There are two scenarios in this thesis which are line of sight (LOS) and none line of sight(NLOS). For the LOS scenario, the transmitter antenna and the receiver antennas must be visible to each other (see Figure 5.3). On the other hand, for NLOS we move transmitter antenna to the area behind a metal block(see Figure 5.6). In our measurement, the communication by USRP is using 2.46 GHz radio frequency with 1MS/s (Symbols/seconds). The results from measurement are shown in the next subsection.

5.2.1 Measurement with Line of Sight

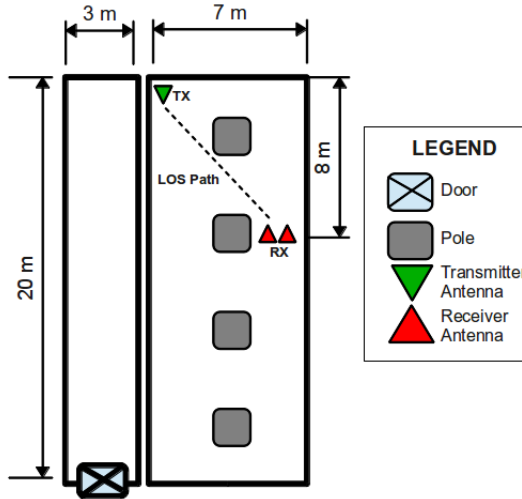


Figure 5.3. Floor plan for line of sight case

Figure 5.4 shows the probability of missed detection for the Average correlation detector, WRAN detector, and SIMO Correlation detector in the measurement with LOS. The settings consist of $N_d = 256$, $N_c = 16$, and $K = 200$.

The settings for the result in Figure 5.5 are almost the same as those in Figure 5.4 except that there are four detectors which are Average correlation detector, WRAN detector, SIMO Correlation detector, and SIMO GLRT detector instead, and that the parameters have been reduced in size to $N_d = 8$, $N_c = 2$, and $K = 500$, respectively.

Both the Average correlation detector and the WRAN detector in LOS measurements (Figure 5.4) and simulation (Figure 5.1) have similar performance, as the difference between them is approximately 6 dB. On the contrary, the performance of the SIMO Correlation detector drops considerably in -12 dB to -10 dB range when compared to the previous simulation. We are not sure about the reason behind it, but we have three hypothesis as a reason for this event. Firstly, the interference may alters the received signal structure. Hence, it worsen the performance of the Average correlation detector and WRAN detector due to the fact that both detectors must know the signal structure of received signal otherwise they are unable to perform correctly. Secondly, our USRP is in a cool state when our program starts measuring the reference noise. However, the measurement take at least 5 hours to finish, so the USRP may have more heat which destroys the signal. Lastly, our SIMO Correlation detector work on an assumption that the noise on both antenna must be uncorrelated, which in practice we cannot verify. Nevertheless, the performance of Average correlation detector and WRAN detector in Figure 5.5 are slightly worse than the simulation in Figure 5.2 with 3 dB

difference between them. In conclusion, SIMO GLRT is the best detector in LOS case while WRAN and SIMO Correlation detectors show similar performance, and Average correlation detector has the worst performance.

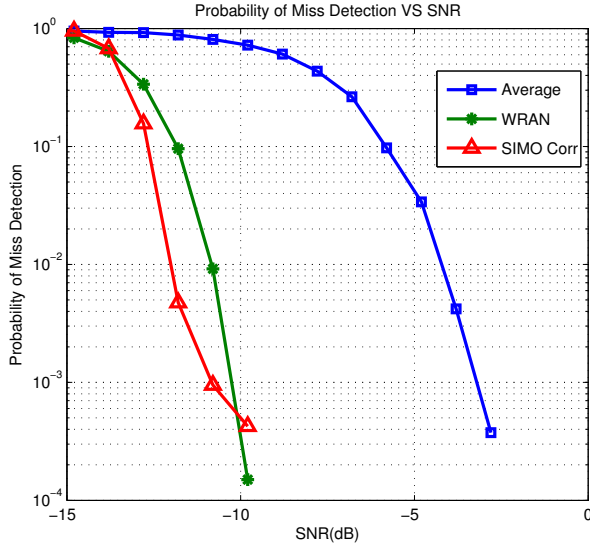


Figure 5.4. LOS-Measurement result with $N_d = 256$, $N_c = 16$, $K = 200$

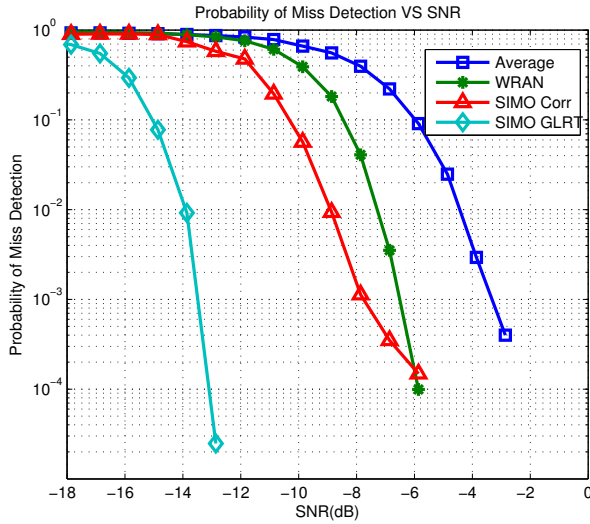


Figure 5.5. LOS-Measurement result with $N_d = 8$, $N_c = 2$, $K = 500$

5.2.2 Measurement with Non Line of Sight

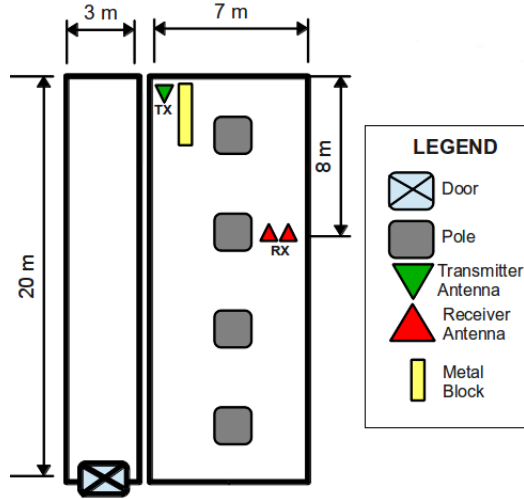


Figure 5.6. Floor plan for non line of sight case

Figure 5.7 shows the probability of missed detection for Average correlation detector, WRAN detector, and SIMO Correlation detector in the measurement with Non-LOS. The settings consist of $N_d = 256$, $N_c = 16$, and $K = 50$.

The setting for the result in Figure 5.8 are almost the same as those in Figure 5.4 except there are four detectors which are Average correlation detector, WRAN detector, SIMO Correlation detector, and SIMO GLRT detector instead, and that the parameters have been reduced in size to $N_d = 8$, $N_c = 2$, and $K = 100$, respectively.

In the Non-LOS case, we are still using the same N_d and N_c as we used in the LOS case. However, we reduce the parameter K because high value of this parameter significantly affect the performance (see Appendix A.1). Generally, the best detector in Non-LOS is still the SIMO GLRT detector while SIMO Correlation, WRAN, Average correlation are the next best detectors in order. It should be noted that the Average correlation detector suffers worst when we change from LOS to Non-LOS. We note that the Average correlation detector has the highest difference in performance at 7 dB between LOS and Non-LOS while the SIMO Correlation detector has the smallest gap between two scenarios at 2 dB. However, we cannot compare the performance between the two scenarios directly due to the parameter K . Nevertheless, the degradation of the Average correlation detector is still obvious.

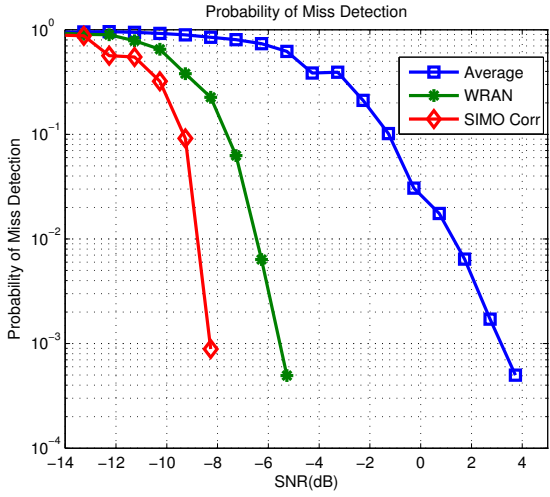


Figure 5.7. NLOS-Measurement result with $N_d = 256$, $N_c = 16$, $K = 50$

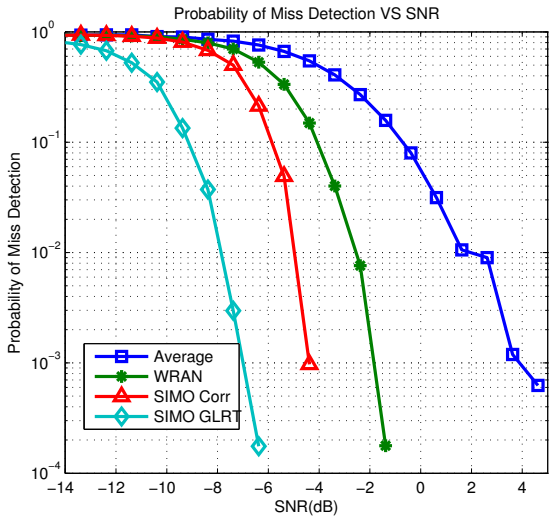


Figure 5.8. NLOS-Measurement result with $N_d = 8$, $N_c = 2$, $K = 100$

Chapter 6

Conclusion and Future Work

6.1 Thesis Conclusion

In conclusion, cognitive radio is an interesting technology which helps improve spectrum utilization without interference to the primary user. In this thesis, we have implemented SIMO Correlation and SIMO GLRT detectors, and compare the performance with other detector through simulations and measurements. Although, there are many kinds of detector for spectrum sensing, but we only compare it with Average correlation detector and WRAN detector. We are using OFDM as the modulation technique for communication, and we have obtained results for each detector in terms of probability of miss detection and SNR. The performance result of every detector in simulation are following the reference paper precisely. Furthermore, both SIMO GLRT detector and SIMO Correlation detector perform very well in simulation. However, in a practical measurement the performance of SIMO Correlation drop harshly on both LOS and NLOS scenarios. Finally, if we ignore the complexity problem of the algorithm then we can conclude that SIMO GLRT is the best detector, which has good performance for both simulations and measurements.

6.2 Future Work

To deepen the analysis, we suggest that one may try to find a better way to reduce the SIMO GLRT algorithm complexity. This should enable handling of larger FFT and CP size as in a real-world environment. Furthermore, one may also make measurements in various kinds of environments such as football field, city downtown, wireless crowded and congested area, etc. This will provide interesting analysis and insights. Moreover, one may implement and compare cooperative sensing algorithms with multi-antenna spectrum sensing in order to get more detailed information about their performance. We believe that by doing above suggestions the system will working better, and could lead to a potential research which may be useful in our daily life.

Bibliography

- [1] Ashish Narayan Pham Nhu Hai. Trends in transition from analogue to digital broadcasting, 2012. Workshop on Digital Broadcasting in Bangkok, Thailand.
- [2] M. Nekovee, T. Irnich, and J. Karlsson. Worldwide trends in regulation of secondary access to white spaces using cognitive radio. *Wireless Communications, IEEE*, 19(4):32–40, 2012.
- [3] M.H. Omar, S. Hassan, and A.H.M. Shabli. Feasibility study of using iee 802.22 wireless regional area network (wran) in malaysia. In *Network Applications Protocols and Services (NETAPPS), 2010 Second International Conference on*, pages 198–202, 2010.
- [4] C. Ciflikli, A. Turgut Tuncer, and A. Tuncay Ozsahin. A new future technology in rural and remote education : Ieee 802.22 cognitive radio based wireless regional access network (wran). In *Application of Information and Communication Technologies, 2009. AICT 2009. International Conference on*, pages 1–5, 2009.
- [5] Santa Rahman, Md. Nahid Hossain, Md. Nizam Sayeed, and M. L. Palash. Comparative study between wireless regional area network (IEEE standard 802.22) and wimax and coverage planning of a wireless regional area network using cognitive radio technology. *International Journal of Recent Technology and Engineering*, 1(6):161–163, 2013.
- [6] R.D. Raut and K.D. Kulat. Sdr design for cognitive radio. In *Modeling, Simulation and Applied Optimization (ICMSAO), 2011 4th International Conference on*, pages 1–8, 2011.
- [7] GNU Radio Website, accessed April 2013.
- [8] Ettus Research, accessed April 2013.
- [9] Khalid Sayood. *Introduction to Data Compression, Third Edition (Morgan Kaufmann Series in Multimedia Information and Systems)*. Morgan Kaufmann, 2005.
- [10] David Tse and Pramod Viswanath. *Fundamentals of Wireless Communication*. Cambridge University Press, 2005.

-
- [11] C. Santivanez, R. Ramanathan, C. Partridge, R. Krishnan, M. Condell, and S. Polit. Opportunistic spectrum access: Challenges, architecture, protocols. In *Proc. 2nd Annual International Wireless Internet Conference (WICON)*, 2006.
- [12] A. Dalvi, P.K. Swamy, and B. B. Meshram. Cognitive radio: Emerging trend of next generation communication system. In *Wireless Communication, Vehicular Technology, Information Theory and Aerospace Electronic Systems Technology (Wireless VITAE), 2011 2nd International Conference on*, pages 1–5, 2011.
- [13] I.F. Akyildiz, Won-Yeol Lee, Mehmet C. Vuran, and S. Mohanty. A survey on spectrum management in cognitive radio networks. *Communications Magazine, IEEE*, 46(4):40–48, 2008.
- [14] A. Shukla, E. Burbidge, and I. Usman. Cognitive radios - what are they and why are the military and civil users interested in them. In *Antennas and Propagation, 2007. EuCAP 2007. The Second European Conference on*, pages 1–10, 2007.
- [15] A.G. Fragkiadakis, E.Z. Tragos, and I.G. Askoxylakis. A survey on security threats and detection techniques in cognitive radio networks. *Communications Surveys Tutorials, IEEE*, 15(1):428–445, 2013.
- [16] Wenkai Wang, Husheng Li, Y.L. Sun, and Zhu Han. Attack-proof collaborative spectrum sensing in cognitive radio networks. In *Information Sciences and Systems, 2009. CISS 2009. 43rd Annual Conference on*, pages 130–134, 2009.
- [17] Pu Wang, Jun Fang, Ning Han, and Hongbin Li. Multiantenna-assisted spectrum sensing for cognitive radio. *Vehicular Technology, IEEE Transactions on*, 59(4):1791–1800, 2010.
- [18] R. Tandra and A. Sahai. Fundamental limits on detection in low snr under noise uncertainty. In *Wireless Networks, Communications and Mobile Computing, 2005 International Conference on*, volume 1, pages 464–469 vol.1, 2005.
- [19] Ian F. Akyildiz, Brandon F. Lo, and Ravikumar Balakrishnan. Cooperative spectrum sensing in cognitive radio networks: A survey. *Physical Communication*, 4(1):40 – 62, 2011.
- [20] D. Bhargavi and C.R. Murthy. Performance comparison of energy, matched-filter and cyclostationarity-based spectrum sensing. In *Signal Processing Advances in Wireless Communications (SPAWC), 2010 IEEE Eleventh International Workshop on*, pages 1–5, 2010.
- [21] Nisha Yadav and Suman Rathi. Spectrum sensing techniques: Research, challenge and limitations 1.

- [22] W. Ejaz, N. ul Hasan, S. Aslam, and Hyung Seok Kim. Fuzzy logic based spectrum sensing for cognitive radio networks. In *Next Generation Mobile Applications, Services and Technologies (NGMAST), 2011 5th International Conference on*, pages 185–189, 2011.
- [23] S. Chaudhari, V. Koivunen, and H.V. Poor. Autocorrelation-based decentralized sequential detection of ofdm signals in cognitive radios. *Signal Processing, IEEE Transactions on*, 57(7):2690–2700, 2009.
- [24] A. Blad, E. Axell, and E.G. Larsson. Spectrum sensing of ofdm signals in the presence of cfo: New algorithms and empirical evaluation using usrp. In *Signal Processing Advances in Wireless Communications (SPAWC), 2012 IEEE 13th International Workshop on*, pages 159–163, 2012.
- [25] Huawei Technologies and UESTC. Sensing scheme for dvb-t. 2006.
- [26] E. Axell and E.G. Larsson. Optimal and sub-optimal spectrum sensing of ofdm signals in known and unknown noise variance. *Selected Areas in Communications, IEEE Journal on*, 29(2):290–304, 2011.
- [27] E. Axell and E.G. Larsson. Multiantenna spectrum sensing of a second-order cyclostationary signal. In *Computational Advances in Multi-Sensor Adaptive Processing (CAMSAP), 2011 4th IEEE International Workshop on*, pages 329–332, 2011.
- [28] Anton Blad, accessed January 2013.
- [29] Gaël Guennebaud, Benoît Jacob, et al. Eigen v3. <http://eigen.tuxfamily.org>, 2010.

Appendix A

Some Additional Graphs

A.1 NLOS Measurement

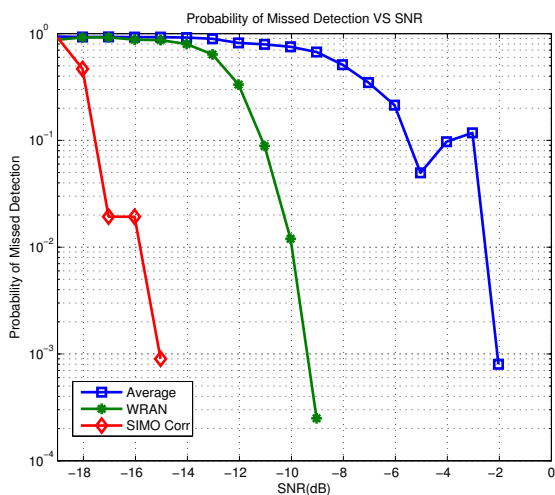


Figure A.1. NLOS-Measurement result with $N_d = 256$, $N_c = 16$, $K = 200$

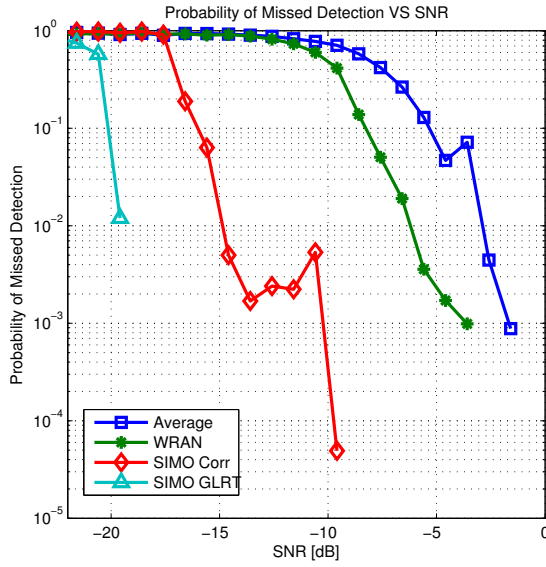


Figure A.2. NLOS-Measurement result with $N_d = 8$, $N_c = 2$, $K = 500$

Appendix B

Source code

B.1 SIMO GLRT

```

for(int theta = 0 ; theta < T ; theta++){
    if(theta == 0)
        K_limit = K;
    else
        K_limit = K-1;
    MatrixXcd block_g(K_limit,N);
    for(int k = 0 ; k < K_limit ; k++){
        for(int index = 0 ; index < N ; index+= Nr){
            block_g(k,index) = data.block[k*T+(index)/Nr+theta];
            block_g(k,index+1) = data.block_multi[k*T+(index)/Nr+theta];
        }
    }
    block_g = block_g*100;
    MatrixXcd phi_hat(N,N);
    phi_hat = block_g.adjoint()*block_g;
    phi_hat = phi_hat / K_limit;
    SelfAdjointEigenSolver<MatrixXcd> eigen_solver(phi_hat,EigenvaluesOnly);
    VectorXd lambda = eigen_solver.eigenvalues();
    double lambda3 = vector_mean(lambda,0,Nc);
    double lambda1 = vector_mean(lambda,Nd,N);
    double lambda2 = vector_mean(lambda,Nc,Nd);
    double sigma2_hat= block_g.cwiseAbs2().sum() / (K_limit*N);
    llr = max(llr, pow(sigma2_hat, N)/(pow(lambda1, N-Nd)+pow(lambda2, Nd-Nc)+pow(
        lambda3, Nc)));
}
m = llr;

```

B.2 SIMO Correlation

```

int Ncorr = K*T;
MatrixXcd input_data(Nr,Ncorr);
MatrixXcd Rxx(Nr,Nr);
for(int index = 0 ; index < Ncorr ; index++){
    input_data(0, index) = data.block[index];
    input_data(1, index) = data.block_multi[index];
}
Rxx = input_data*input_data.adjoint();
Rxx = Rxx/Ncorr;
SelfAdjointEigenSolver<MatrixXcd> eigen_solver_corr(Rxx,EigenvaluesOnly);
VectorXd lambda_corr = eigen_solver_corr.eigenvalues();
m = lambda_corr(1)/lambda_corr.sum();

```